

## Heat-sensitive polyacrylamide nanoparticle for cancer treatment

Marta d'Amora<sup>1†\*</sup>, Patrizia Colucci<sup>2†</sup>, Alice Usai<sup>2</sup>, Elena Landi<sup>2</sup>, Lieselot Deleye<sup>1</sup>, Luciana Dente<sup>2</sup>, Francesco De Angelis<sup>1</sup>, Vittoria Raffa<sup>2\*</sup>, Francesco Tantussi<sup>1</sup>

<sup>1</sup>*Istituto Italiano di Tecnologia, Via Morego 30, 16163 Genova, Italy*

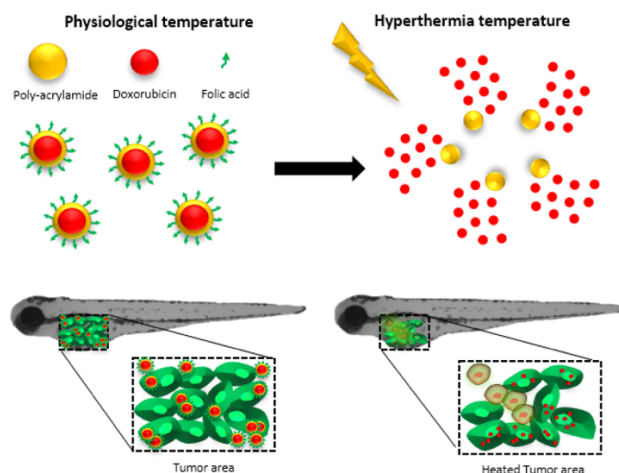
<sup>2</sup>*Department of Biology, University of Pisa, S.S. 12 Abetone e Brennero 4, 56127 Pisa, Italy;*

Submitted: August 31, 2020

Accepted October 9, 2020

Published: October 12, 2020

### Graphical abstract



Folic acid-conjugated polyacrylamide nanoparticles encapsulating doxorubicin were injected in zebrafish embryos. At hyperthermia temperature, the nanoparticles released doxorubicin into the xenografted cells, arresting the tumor.

### Abstract

Several nanomedicine-based platforms, including polymeric micelles, dendrimers, and liposomes, have been developed and explored for targeted delivery of therapeutics in cancer. These nanoparticles are capable of delivering selectively antineoplastic agents to the tumor, reduce the untoward toxicity, and improve the therapeutic effect. In the present study, we propose new thermosensitive polyacrylamide-based nanoparticles as polymer-based drug carriers. Polyacrylamide has a controllable swelling temperature, which enables a rapid release of an encapsulated drug above certain temperatures. PAA-NP was synthesized then functionalized with folic acid to improve selective targeting. Then doxorubicin, an antineoplastic agent, was encapsulated inside of the polymeric core. Our data show that these nanoparticles have a sol-gel transition temperature of 41°C. We investigated the effects of the folic acid functionalized PAA nanoparticles on HeLa cells both in vitro and in vivo, and on zebrafish larvae xenografted with human pancreatic cancer cell line Mia Paca-2. Functionalized NPs were internalized in a short time by the cancer cells, mainly localizing in the lysosomes. In vitro and in vivo cytotoxicity studies indicated high viability of cells treated with functionalized nanoparticles encapsulating doxorubicin by signaling a minor release of doxorubicin at physiological temperatures. Conversely, at the temperature of 41 °C, they trigger apoptosis of the xenografted cells, resulting in a strong arrest of the increase of the tumor area. Our results suggest that the heat-activated DOX:PAA-NP-FA could be used to implement combined therapies for the local treatment of solid cancers.

### Keywords

Nanoparticles, polyacrylamide, folic acid, thermosensitive, doxorubicin, triggered drug release, solid cancer.

\* Corresponding authors: Marta d'Amora [Marta.Damora@iit.it](mailto:Marta.Damora@iit.it), Vittoria Raffa [Vittoria.Raffa@unipi.it](mailto:Vittoria.Raffa@unipi.it)

† equally contributed

## Rationale and Purpose

The purpose of this study is to develop heat-sensitive, and FA functionalized polyacrylamide nanocarriers capable of the efficient delivery and triggered release of doxorubicin by thermal modality to solid tumors. The rationale behind this study is to obtain a sol-gel transition temperature of polyacrylamide above the physiological temperature (37°C) and to trigger the doxorubicin release by increasing the temperature locally in cancer cells overexpressing FA until 41°C. To achieve the above goal, polyacrylamide is copolymerized with acrylamide (AA) and allylamine (AH). Copolymerization increases the sol-gel temperature of polyacrylamide, and the amine groups of allylamine provide more sites for the functionalization with FA. The conjugation of the copolymer with FA allows specifically targeting cancer cells of different solid tumors. In fact, most of the solid tumors, including testicle, prostate, pancreas, brain, lung, breast, ovary, and kidney cancer, overexpress the FA receptor.

## Introduction

Cancer is a worldwide major public health problem in the 21<sup>st</sup> century, responsible for one in four deaths [1]. To date, conventional chemotherapy presents a major strategy for the treatment of solid tumors, particularly aggressive and rapidly growing form of cancers. However, chemotherapeutics lack efficient specificity toward tumor and healthy tissues, causing systemic toxicity and innumerable adverse effects in already debilitated patients [2, 3]. To overcome the drawbacks of anticancer drugs, the development of different specific nanocarriers represents an appropriate approach to transfer and release anticancer drugs in a selective and controlled manner to the target site, increasing the therapeutic efficacy and reducing systemic side effects [4-11]. These nanocarriers include metallic nanoparticles [12], dendrimers [13], polymeric micelles [14], carbon-based nanoparticles [15], liposomes [16] and polymeric nanoparticles [17]. Among these platforms, polymeric nanoparticles have gained importance due to their unique characteristics, such as their high drug-loading capacity, stability, tunable physicochemical properties, sustained drug release, biodegradability, and

biocompatibility [18-21]. Recent investigations have focused on stimulus-responsive polymeric systems due to the possibility to release drugs upon internal or external triggers (temperature, pH, redox potential) [22-25]. In particular, thermo-responsive polymeric nanoparticles represent smart systems for the controlled release of anticancer agents into the tumor area, which is simultaneously heated by a thermal modality [26-28]. Heat-sensitive polymers are designed to maintain the drug entrapped around physiological temperature (37°C) and fast release it locally in the heated tumor (40–43°C) [29-34]. However, not all the thermosensitive carriers possess good stability at physiological temperature. For instance, different lysolipid-containing thermosensitive liposomes, including the commercially available formulation known as ThermoDox [35], present a decrease in the thermal sensitivity and a massive release of drugs at the physiological condition when these nanosystems are administered in vivo [36, 37]. Polyacrylamide (PAA) is one of the most studied heat-sensitive polymers; it is biologically and chemically inert, optically transparent, and biodegradable [38-40]. PAA achieves a sol-gel transition temperature at about 32°C that can be increased by copolymerization with hydrophilic or hydrophobic monomers [41-43]. Thus, in this work, we have successfully developed folic acid (FA)-functionalized PAA nanoparticles as a novel nanosystem capable of efficient delivery and temperature-triggered release of doxorubicin (DOX) to cancer cells overexpressing the folate receptor. Our nanoparticles were synthesized through polymerization of N-isopropyl-acrylamide, acrylamide, and allylamine, which result in the formation of swellable PAA systems. PAA-NP was loaded with DOX. Moreover, their surface was decorated with FA that can lead to targeted site-specific therapy of solid tumors. FA functionalized, and DOX-loaded nanoparticles (DOX:PAA-NP-FA) were characterized by different techniques and evaluated in vitro in terms of cellular uptake and cytotoxic effects on HeLa cells. At physiological temperatures, our spherical and DOX-containing nanoparticles showed no toxicity in cancer cells expressing the folate receptor. In addition, we investigated the intracellular localization of DOX:PAA-NP-FA and found that they were mainly localized into the lysosomes. We also investigated the effectiveness of the nanoparticles in vivo on

zebrafish larvae xenografted with human pancreatic cancer cell line Mia PaCa-2. After increasing the temperature to 41°C, we observed a significant high doxorubicin release, demonstrating their temperature sensitivity. Our results show a high potential of DOX:PAA-NP-FA for efficiently triggered drug delivery and potential eradication of cancer cells in solid tumors.

## Materials and Methods

### Nanoparticle synthesis

#### *Synthesis of PAA-NPs containing doxorubicin (DOX:PAA-NP)*

The acrylic nanoparticles are polymeric organic particles composed of N-isopropyl acrylamide (NIPA), acrylamide (AAM), allylamine hydrochloric acid (AH), and N,N-methylene bisacrylamide (BIS) as a cross-linking agent. They were synthesized by optimizing the radical polymerization protocol developed by Rahimi and colleagues [43] using ammonium persulfate (APS) as initiator, sodium dodecyl sulfate (SDS) as surfactant, and N,N,N',N'-tetramethyl ethylene diamine (TEMED) as an activator. 22.2% w/v of NIPA (Sigma-Aldrich®), 2.86% w/v of AAM (Sigma-Aldrich®), 7.6% w/v of AH (Sigma-Aldrich®), and 26.2% v/v of 2% BIS (Sigma-Aldrich®) were dissolved in 10 mL of de-ionized water previously purged with argon at room temperature and under stirring. 1.15% v/v of SDS (Sigma-Aldrich®) was added, and the solution was purged with argon for 30 minutes. 4% v/v of 20 µg/mL doxorubicin (Sigma-Aldrich®) was dissolved before to stop the argon flow, and 1.56% w/v of APS (Sigma-Aldrich®) and 2% v/v of TEMED (Sigma-Aldrich®) were added. Finally, de-ionized water purged with argon was added to the final volume of 20 mL, and the reaction was carried out at room temperature for 3 hours under continuous stirring in darkness. Dialysis was performed, transferring the sample into a 10 kDa cut-off membrane kept in de-ionized water under stirring and replacing with new water each hour per four times. Finally, the sample was concentrated by a centrifuge using a 30 kDa Vivaspin® tube (Sartorius Stedim Biotech) and kept at 4°C.

#### *Functionalization with folic acid (DOX:PAA-NP-FA)*

The reaction was carried out adding 1 mg/mL of FA solution (Sigma-Aldrich®) to the NPs

and mixing the suspension for 2 hours in ice under stirring. Finally, the unbounded vitamin was removed by centrifugation (15000 rpm for 3 hours with 3 washing steps), and the sample was concentrated using a 30 kDa Vivaspin® tube.

### 2.2 Nanoparticle characterization

The doxorubicin concentration and the lower critical solution temperature (LCST) determination were estimated in a range between 25–50°C by measuring the absorbance at 480 nm and at 650 nm, respectively.

The structural morphology of the synthesized DOX:PAA-NP-FA were examined by transmission electron microscopy. Samples were suspended in distilled water, placed on copper grids, and dried overnight. All samples were examined under a JEOL 100XI transmission electron microscope. Moreover, to study the nanoparticles' diffusion behavior in solution, dynamic light scattering (DLS) measurements were performed using a Zetasizer Nano 3600 from Malvern Instruments. The hydrodynamic diameter calculated from the diffusion coefficient depends on the size and shape of the particles.

### In vitro biological studies

#### *Cell culture*

For in vitro studies, HeLa (cervical epithelial cancer cells) cells were cultured in Dulbecco's Modified Eagle Medium (DMEM) (Thermo Fisher Scientific) supplemented with 10% fetal bovine serum (FBS) (Thermo Fisher Scientific), and 1% penicillin/streptomycin (Thermo Fisher Scientific) in a humidified incubator at 37°C in an atmosphere of 5% CO<sub>2</sub>. Cells were passaged at 80% confluency, split 1:10 in fresh medium, and discontinued after passage 15.

#### *Toxicity assessment*

The cytotoxic effects of DOX:PAA-NP-FA on HeLa cells were evaluated by WST1 assay (Roche Applied Sciences). Briefly, HeLa cells were seeded at a density of 5000 cells per well in 96-well plates and cultured overnight at 37°C in a humidified atmosphere with 5% CO<sub>2</sub>. Then, the cells were exposed for 48 and 72 hours to polymeric nanoparticles without doxorubicin or different concentrations of DOX:PAA-NP-FA (0.01, 0.1 and 0.5 µM DOX equivalence) or free DOX (0.01, 0.1, and 0.5 µM). A culture medium containing 10% of dimethyl sulfoxide (DMSO) was used as a

positive control, while DMEM alone as a negative one. A volume of 10  $\mu$ l WST-1 reagent was added to each well. After 2 hours of incubation in the same conditions, cell viability was determined by optical absorption at 450 nm using a microplate spectrophotometer with a reference wavelength of 690 nm. All measurements were performed in triplicate. Data collected were expressed as the mean value  $\pm$  standard deviation (mean  $\pm$  SD). One-way analysis of variance (ANOVA) was used to make a comparison among groups,  $p < 0.05$  was considered significant.

#### *Cellular uptake and intracellular localization*

To visualize the cellular uptake behaviour of DOX:PAA-NP-FA, HeLa cells were seeded on chambered coverglass (Thermo Scientific Nunc Lab-Tek II) and cultured in DMEM at 37 °C in a humidified atmosphere with 5% CO<sub>2</sub> overnight. Then, cells were treated with DOX:PAA-NP-FA (0.1 and 0.5  $\mu$ M DOX equivalence) or free DOX (0.5  $\mu$ M) for 24 h. After incubation, the cells were washed three times with phosphate-buffered saline (PBS) (0.1 M, pH 7.4), and stained for 15 min with a solution of Hoechst 33342 (5  $\mu$ g mL<sup>-1</sup>; Sigma-Aldrich) or LysoTracker Green (75 nM; Life Technologies) to visualize the nuclei and lysosomes respectively. Finally, the cells were washed three times and filled with PBS (0.1 M, pH 7.4), and the cellular uptake and intracellular distribution of DOX:PAA-NP-FA were visualized by a laser scanning confocal microscope and a plan Apo 20X DIC M objective (Nikon A1R, Japan).

#### *In vivo biological studies*

##### *Animal handling*

Animals were handled in compliance with protocols approved by the Italian Ministry of Public Health and the local Ethical Committee in conformity with EU legislation (Directive 2010/63/EU). Zebrafish embryos were obtained by natural mating of wild-type fishes and maintained in the incubator at 28°C, according to the ZFIN procedures. Before any injection, embryos were anesthetized in 0.02% tricaine.

##### *Cell culture and staining*

Human pancreatic cancer cell line Mia PaCa-2 were cultured in DMEM supplemented with 10% FBS, 100 U/mL penicillin, and 100  $\mu$ g/mL streptomycin. Cells were incubated at 37°C in a saturated humidity atmosphere with 5% CO<sub>2</sub>. Cells were detached at 80% confluence with 0.25% (w/v) trypsin –0.53 mM EDTA solution

and stained with 10  $\mu$ g/mL CM-Dil for 15 minutes at 37°C followed by 15 minutes on ice in darkness. Cells were washed and centrifuged three times in Dulbecco's phosphate-buffered saline (DPBS) and resuspended in DPBS supplemented with 10% FBS to a final concentration of 100 cells/nL.

##### *Tumor cells microinjection and imaging*

Embryos were anesthetized in 0.02% tricaine and put on 1% agarose, laying on the right side. Four nanoliters (around 400 cells) of stained cell suspension were injected into the yolk at the left side of 48 hpf (hours post fertilization) embryos, using a heat-pulled needle connected to a PV830 Pneumatic PicoPump air microinjector. Xenografted embryos were maintained at 35°C in E3 medium supplemented with 100 U/mL penicillin and 100  $\mu$ g/mL streptomycin (E3 Pen/Strep medium) for two hours, and the presence of DiI fluorescence was checked using the tetramethylrhodamine channel of a Nikon Ti-Eclipse microscope. Subsequently, embryos were randomly distributed in 24-well plates (one embryo/well) and anesthetized with a 0.02% tricaine in E3 Pen/Strep medium solution. Bright-field and TRITC images of the fluorescent dye area at the left side of the embryos were acquired at 2 hpi (hours post-injection) and finally analyzed using the ImageJ software.

##### *Nanoformulation efficacy assessment*

Two hours after the xenograft, four nanoliters of 2.5  $\mu$ g/mL of DOX or DOX:PAA-NP-FA or de-ionized water were injected into the yolk of 48 hpf xenografted embryos, using a heat-pulled needle connected to a PV830 Pneumatic PicoPump air microinjector. Before any injection, embryos were anesthetized in 0.02% tricaine and put on 1% agarose, lying on the right side. Embryos were maintained at 35°C in E3 Pen/Strep medium for 1 hour and then transferred into a 41°C bath for 5 minutes. Bright-field and TRITC images of the DiI-stained area at the left side of the embryos were acquired after 24 and 48 hpt (hours post-treatment). At 48 hpt, the embryos were fixed with 4% PFA for 1 hour at RT, then incubated with Hoechst 10  $\mu$ g/mL for 2 hours at RT. Xenografts were acquired by Nikon A1 confocal microscope at 60 $\times$  magnification with 5  $\mu$ m interval z-stacks. Quantification analysis of both tumor area and pyknotic cells were performed using the ImageJ software.

## Results and discussion

### Characterization of DOX:PAA-NP

DOX:PAA-NP were synthesized by modifying the protocol of Rahimi [32] to obtain particles with a hydrodynamic size of 50 nm. The DLS measurements showed an average diameter of 50 nm and a concentration of around  $1.04 \times 10^8$  particles per  $\mu\text{l}$  (Figure 1A, black line). The size distribution of particles was also confirmed by TEM observations. The DLS measurements of DOX:PAA-NP-FA showed that the functionalization with folic

acid does not affect the stability and dimensions of our acrylic particles (Figure 1A, red line).

To quantify the doxorubicin loaded into the NPs, a spectrophotometer assay was carried out showing a concentration of  $5.6 \mu\text{g/mL}$ . Then, in order to evaluate the temperature at which the phase transition occurs, a second spectrophotometer assay was performed by measuring the absorbance at different temperatures. The results showed a solid-gel phase transition between  $40\text{--}45^\circ\text{C}$ , which allows us to perform a drug release in a time and physically controlled manner (see Figure 1).

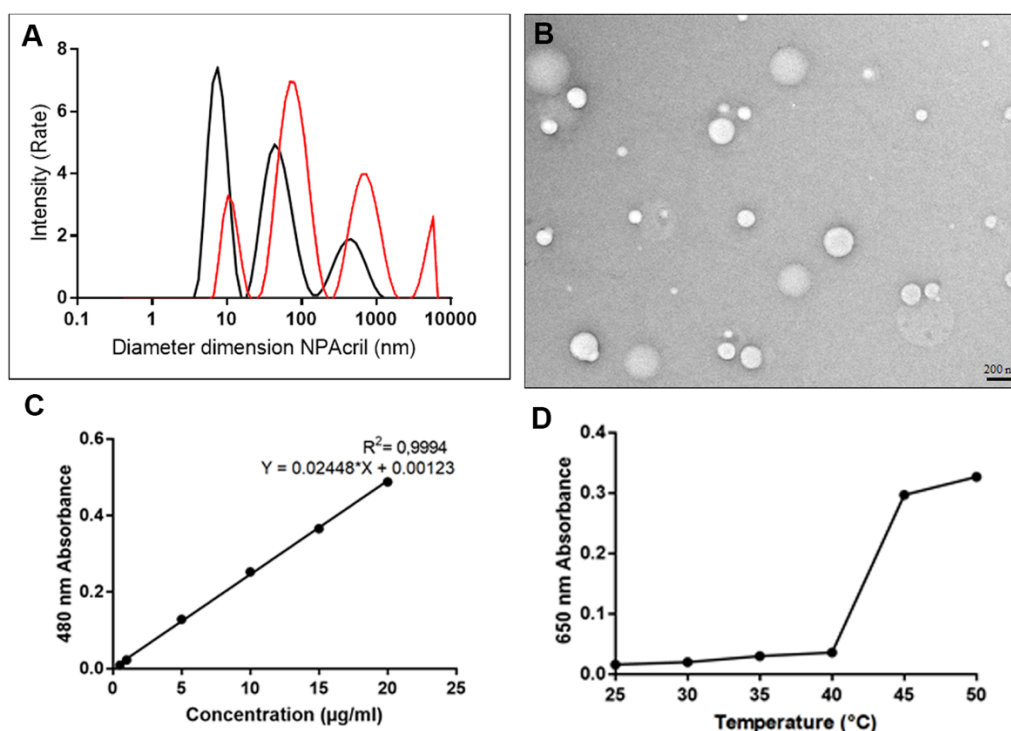


Figure 1. (A) Hydrodynamic size distribution of acrylic nanoparticles before (black) and after (red) functionalization with folic acid. The peaks at 10 and 50 nm highlight the presence of particle populations with different dimensions, while the 800 nm peak could represent clustered particles. (B) Transmission electron microscope analysis. These observations confirm the dimensional distributions of particles. (C) Calibration curve for the determination of the doxorubicin content into the nanoparticles. (D) Lower critical solution temperature determination.

### In vitro studies

#### Toxicity assessment

The biosafety of the nanocarriers is very important in the development of biocompatible drug delivery systems. Hence, the effects of DOX:PAA-NP-FA was evaluated against HeLa cells by the colorimetric WST1 assay. HeLa cells were treated for 48 and 72 hours, with increasing concentrations of nanoparticles and free doxorubicin. Moreover, cells were also exposed to blank polymeric nanoparticles (no

doxorubicin), cell medium (negative control), and DMSO (positive control). Notably, the cellular viability of cells treated with DOX:PAA-NP-FA was greater than 80% at the equivalent concentrations of doxorubicin of 0.01, 0.1 to 0.5  $\mu\text{M}$  (Figure 2), demonstrating the negligible cytotoxic effects of our nanoparticles toward cancer cells at physiological conditions. In the meantime, cells treated with free doxorubicin showed a decrease in the cellular viability under the same conditions (0.01, 0.1, 0.5  $\mu\text{M}$ ). HeLa cells

presented a high sensitivity to free doxorubicin, reaching 50% of cell viability at the highest concentration used. Our polymeric nanoparticles without doxorubicin did not produce any reduction in the cell viability at both time points and the cellular medium. On the other side, as a positive control, HeLa cells

exposed to DMSO presented a decrease in the viability, reaching a value of 30% after 72 hours of treatment. These results indicated that the developed nanoplatforms could retain the chemotherapeutic agent at body temperature, reporting their suitability as biocompatible and stable drug carriers.

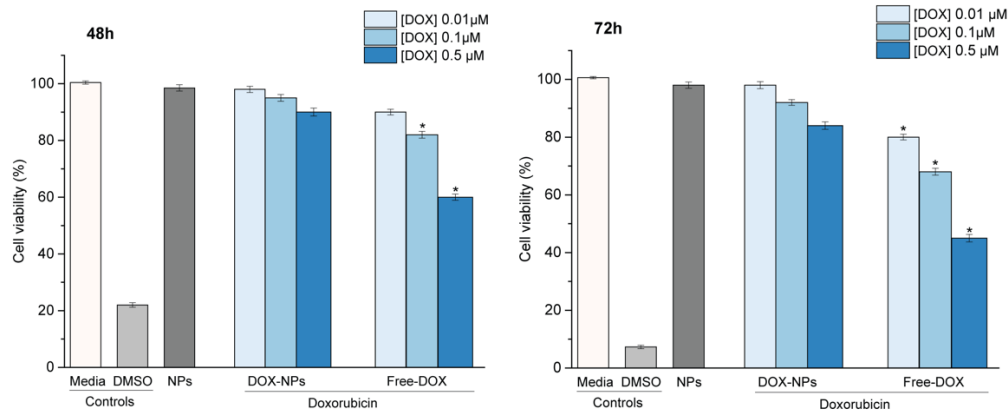


Figure 2. Cellular viability of HeLa cells treated with medium alone, polymeric nanoparticles (NPs) without DOX (NPs), DOX:PAA-NP-FA (DOX NPs), free DOX and DMSO for 48 and 72 hours. Data were expressed as the mean  $\pm$  standard error as calculated from three independent experiments (\* $p < 0.05$ ).

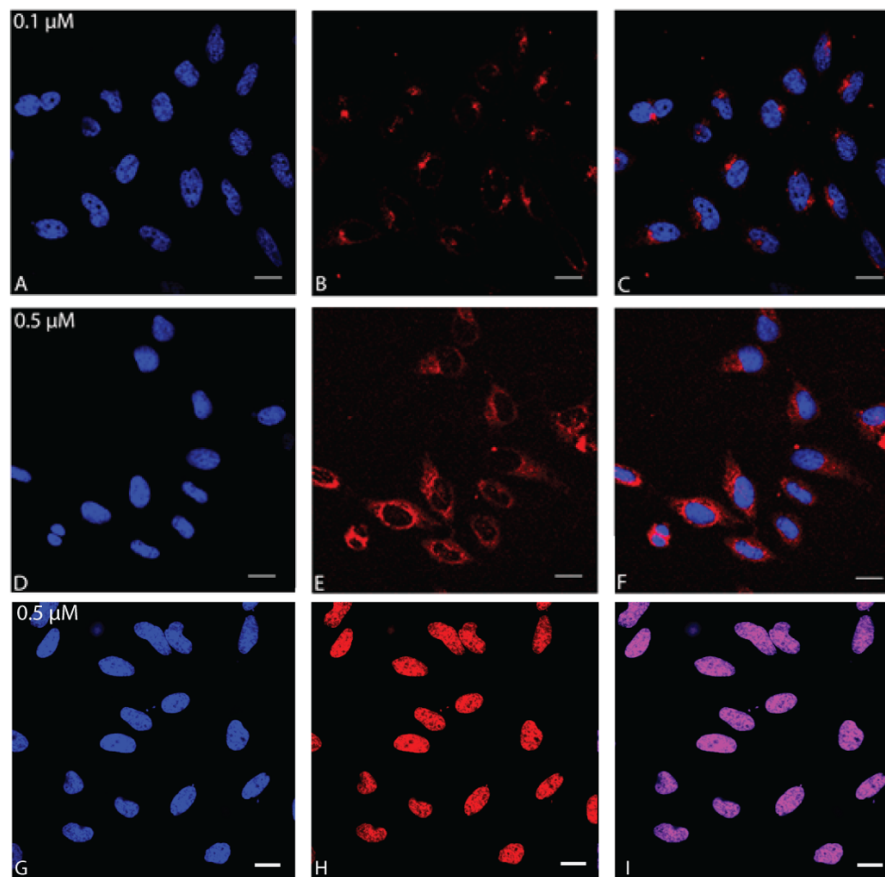


Figure 3. Confocal live images of HeLa cells incubated for 24 hours with DOX:PAA-NP-FA (0.1 and 0.5 μM DOX equivalence) or DOX (0.5 μM). (A, D and G) Cell nuclei stained by Hoechst 33342 (blue); (B and E), intracellular distribution of nanoparticles (DOX, red); (H) distribution of free DOX, (red); (C, F and I) overlays of all images (merged). Scale bars=10 μm.

### Cellular uptake and intracellular localization

The delivery of therapeutic agents into the cytoplasm is critical for successful cancer therapy. Therefore, we investigated the cellular uptake behavior and intracellular localization of our nanoparticles. HeLa cells were treated with DOX:PAA-NP-FA or free DOX and were observed after 24 hours of treatment by confocal microscopy, thanks to the intrinsic fluorescence properties of doxorubicin. As shown in Figure 3C, the DOX:PAA-NP-FA were efficiently internalized in cancer cells by endocytosis and were predominantly distributed in the cytoplasm around the nuclei. Moreover, we investigated in more detail the intracellular localization of DOX:PAA-NP-FA. To study the possible distribution of NPs in vesicular compartments, HeLa cells treated with DOX:PAA-NP-FA were stained with a

lysosome specific dye (LysoTracker Green). As shown by the merged confocal live images (Figure 4), the red intrinsic fluorescence of the doxorubicin overlapped with the LysoTracker Green (yellow signal), indicating that DOX:PAA-NP-FA accumulated totally in the lysosomes. When the DOX:PAA-NP-FA concentration increased (Figure 3F), a remarkable increase in fluorescence intensity of doxorubicin was observed. On the other hand, free doxorubicin presented its typical localization in the cell nuclei (Figure 3I). Our results indicated a high uptake of DOX:PAA-NP-FA by cancer cells. Moreover, the different uptake patterns of DOX:PAA-NP-FA in comparison to free doxorubicin, demonstrated the stability of the intact DOX:PAA-NP-FA into the cells without being subjected to degradation.

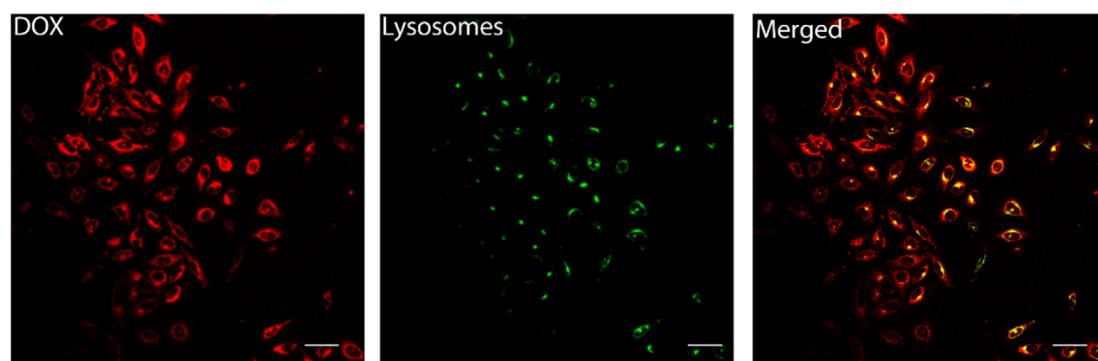
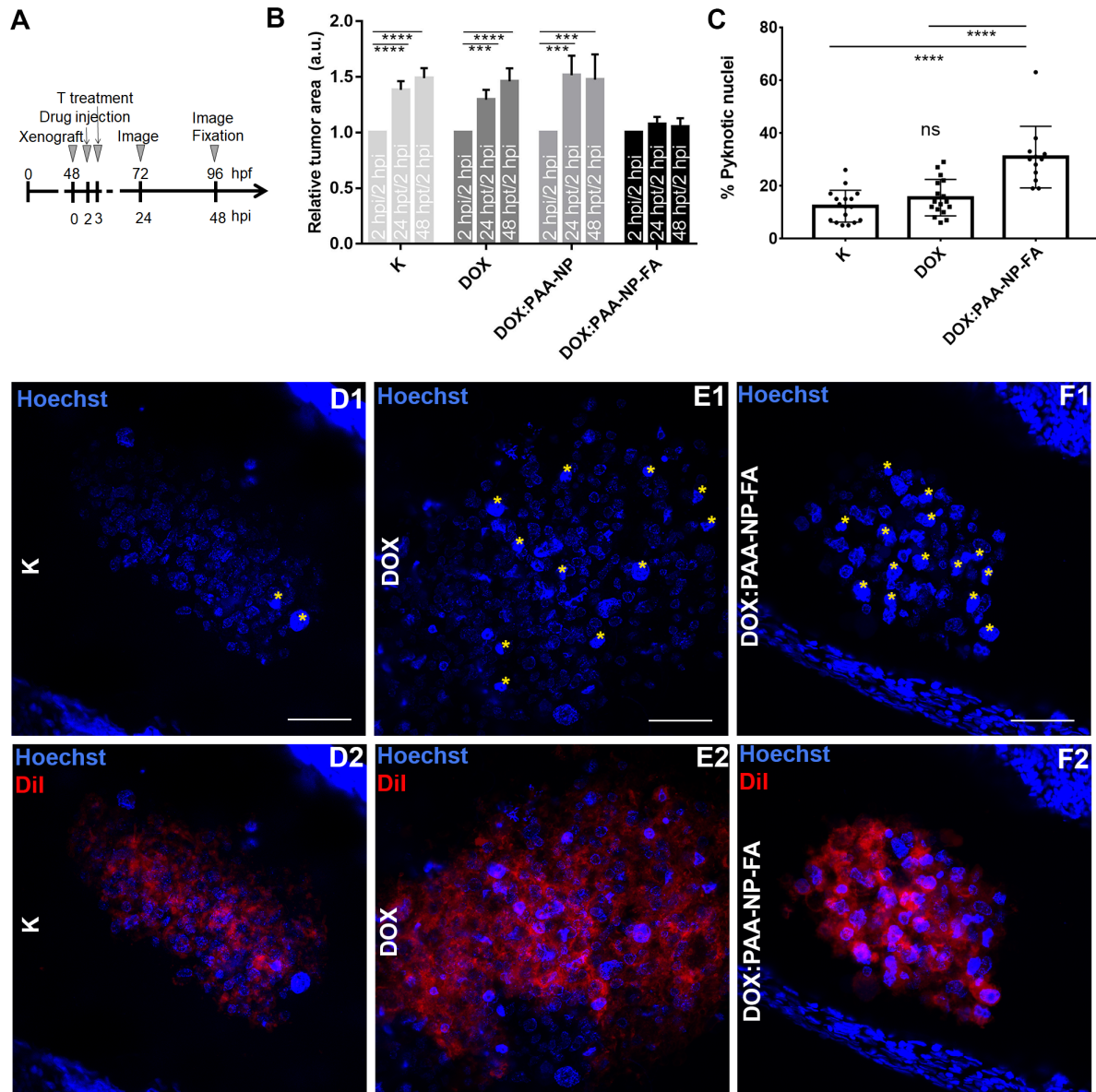


Figure 4. Confocal live images of HeLa cells incubated for 24 hours DOX:PAA-NP-FA (0.5  $\mu$ M DOX equivalence). The images from left to right show the intracellular distribution of nanoparticles (DOX, red), the lysosomes stained with LysoTracker Green (green), and overlays of all images (merged). Scale bars = 20  $\mu$ m.

### In vivo studies

The therapeutic efficacy of the nanoformulation was evaluated by injecting saline or DOX, DOX:PAA-NP, or DOX:PAA-NP-FA into 48 hpf zebrafish embryos, previously xenografted with DiI-labelled Mia PaCa-2 cancer cells. Embryos were held at 41°C for 5 minutes to promote doxorubicin release from the polymeric matrix. The exposure of the embryos to the temperature did not induce death or malformations of embryos (100% of embryos survived at 40, 41, and 42°C for 2-5 minutes, n=18 for each condition). Bright-field and TRITC images of the left side of each embryo were acquired before treatment (at 2 hpi) and after treatment (at 24 and 48 hpt), and the DiI-stained areas were analyzed and normalized with respect to the first time point (2 hpi). In the absence of any treatment (K), the DiI-stained area showed a statistically

significant increase over time. The block or inversion of this tendency was considered a hallmark of the chemotherapy effect. The analysis of the DiI-stained areas of the control group showed a statistically significant increase in the size of the relative areas over time as expected, and the same result was obtained treating the cells with DOX or DOX:PAA-NP. On the contrary, no statistically significant differences were observed in the size of fluorescent areas in the DOX:PAA-NP-FA treatment group over time (Figure 5B). Moreover, the analysis of pyknotic nuclei revealed a significant increase of apoptosis in the DOX:PAA-NP-FA treatment group with respect to the DOX and control groups (Figure 5C-F). All evidence suggests a strong ability of these particles to be internalized into the cells, exploiting the presence of the FA on their surface, and promote the anticancer activity of the doxorubicin cargo.



**Figure 5.** (A) Experimental timeline. Mia PaCa-2 cancer cells and saline or DOX or DOX:PAA-NP were injected into the yolk sac of 48 hpf zebrafish embryos. Imaging of DiI-stained areas at 2 hpi and 24 and 48 hpi was performed and the embryos were fixed at 48 hpi and Hoechst counterstained. (B) Nanodevice efficacy assessment. The graph represents the analysis of the relative DiI-stained areas recorded at 2 hpi, 24 hpi and 48 hpi and normalized with respect to the first time point (2 hpi). The DOX:PAA-NP, the DOX, and the control groups show a statistically significant increase in tumor area over time with respect to the DOX:PAA-NP-FA group.  $n \geq 30$  from three independent assays. (C) Percentage of pyknotic nuclei of Mia PaCa-2 cancer cells recorded at 48 hpi. A statistically significant increase in the apoptosis rate in the DOX:PAA-NP-FA group with respect to the DOX and the control groups was observed ( $n \geq 12$  from three independent assays). Data were expressed as mean  $\pm$  SEM and analyzed by ANOVA test followed by Bonferroni correction (\*\*  $p < 0.01$ ; \*\*\*  $p < 0.001$ ; \*\*\*\*  $p < 0.0001$ ). (D) Confocal images of control xenografts, (E) xenografts treated with DOX (F), and xenografts treated with DOX:PAA-NP-FA. Stars denote cells with pyknotic nuclei.

## Conclusion

In this study, we propose an approach of precision nanomedicine, combining the principles of physical-activation and active targeting of the drug release. More specifically, we developed FA-functionalized thermosensitive polyacrylamide platforms encapsulating doxorubicin by copolymerization of PAA, acrylamide, and allylamine. These nanoparticles presented a swelling temperature above the physiological conditions (at 41°C), with high stability and minimized drug release at body temperature, and a quick release of the drug in response to changes in the local temperature (hyperthermia temperature) both in vitro (HeLa cells) and in vivo (xenografted zebrafish).



The quick release of the chemotherapeutic drug by thermic responsiveness denotes that our thermosensitive carriers will be powerful platforms for solid tumor treatment, considering that the aggressive release of chemotherapeutic drugs is needed to inhibit tumor proliferation. Moreover, our platforms are functionalized with FA and consequently possess a high selective target ability for solid tumors. This conjugation increases the therapeutic efficiency of our nanoparticles, reducing potential side effects. This is another advantage in comparison to other drug delivery systems. In fact, several nanocarriers, including the lipid-based one, can reach the tumor area by passive targeting, entering the lymphatic circulation. However, this approach presents different limitations, including a problematic control of the system, leading to a non-specific accumulation in the spleen and liver and multidrug resistance. Our systems do not possess these defects since they actively target the tumor area and release doxorubicin in the cancer cells, which is triggered by the increase of temperature. In conclusion, our FA functionalized thermosensitive polyacrylamide nanoparticles represent new powerful temperature-triggered and active tumor-targeting drug delivery systems.

## Funding

Fondazione Pisa (project 114/16) and PRA 2018-2019 (UNIFI, bandi di Ateneo) are greatly acknowledged for funding.

## Acknowledgments

The authors wish to thank Dr. Riccardo Carzino for the DLS measurements, Nikon Imaging Center@IIT and IIT Nanochemistry department for access to facilities, Dr. Martina Giannaccini and Matteo Baggiani for supporting nanoparticle synthesis. We acknowledge the CIME (Centro Interdipartimentale di Microscopia Elettronica) for TEM imaging.

## Conflict of Interests

The authors declare no conflicts of interest. For a signed statement, please contact the journal office: [editor@precisionnanomedicine.com](mailto:editor@precisionnanomedicine.com)

Quote this article as d'Amora M, Colucci P, Usai A, Landi E, Deleye L, Dente L, De Angelis F, Raffa V, Tantussi F, Heat-sensitive polyacrylamide nanoparticle for cancer treatment, *Precis. Nanomed.* 2020;3(4):666-676, <https://doi.org/10.33218/001c.17629>

## References

- [1] B. Pulverer, L. Anson, C. Surridge, and L. Allen, "Cancer," *Nature*, vol. 411, pp. 335-335, 2001/05/01 2001.
- [2] R. L. Siegel, K. D. Miller, and A. Jemal, "Cancer statistics, 2018," vol. 68, pp. 7-30, Jan 2018.
- [3] P. S. Steeg, "Targeting metastasis," *Nature Reviews Cancer*, vol. 16, pp. 201-218, 2016/04/01 2016.
- [4] I. Hamad, O. Al-Hanbali, A. C. Hunter, K. J. Rutt, T. L. Andresen, and S. M. Moghimi, "Distinct Polymer Architecture Mediates Switching of Complement Activation Pathways at the Nanosphere–Serum Interface: Implications for Stealth Nanoparticle Engineering," *ACS Nano*, vol. 4, pp. 6629-6638, 2010/11/23 2010.
- [5] H. Wang, H. Xie, J. Wu, X. Wei, L. Zhou, X. Xu, et al., "Structure-Based Rational Design of Prodrugs To Enable Their Combination with Polymeric Nanoparticle Delivery Platforms for Enhanced Antitumor Efficacy," *Angewandte Chemie International Edition*, vol. 53, pp. 11532-11537, 2014.
- [6] A. Schroeder, D. A. Heller, M. M. Winslow, J. E. Dahlman, G. W. Pratt, R. Langer, et al., "Treating metastatic cancer with nanotechnology," *Nature Reviews Cancer*, vol. 12, pp. 39-50, 2012/01/01 2012.
- [7] Y. F. Tan, L. L. Lao, G. M. Xiong, and S. Venkatraman, "Controlled-release nanotherapeutics: State of translation," *Journal of Controlled Release*, vol. 284, pp. 39-48, 2018/08/28/ 2018.
- [8] J. K. Patra, G. Das, L. F. Fraceto, E. V. R. Campos, M. d. P. Rodriguez-Torres, L. S. Acosta-Torres, et al., "Nano based drug delivery systems: recent developments and future prospects," *Journal of Nanobiotechnology*, vol. 16, p. 71, 2018/09/19 2018.
- [9] Y. Du, W. Ren, Y. Li, Q. Zhang, L. Zeng, C. Chi, et al., "The enhanced chemotherapeutic effects of doxorubicin loaded PEG coated TiO<sub>2</sub> nanocarriers in an orthotopic breast tumor bearing mouse model," *Journal of Materials Chemistry B*, vol. 3, pp. 1518-1528, 2015.

- [10] H. Wang, Z. Lu, L. Wang, T. Guo, J. Wu, J. Wan, et al., "New Generation Nanomedicines Constructed from Self-Assembling Small-Molecule Prodrugs Alleviate Cancer Drug Toxicity," *Cancer Research*, vol. 77, pp. 6963-6974, 2017.
- [11] H. Wang, J. Wu, K. Xie, T. Fang, C. Chen, H. Xie, et al., "Precise Engineering of Prodrug Cocktails into Single Polymeric Nanoparticles for Combination Cancer Therapy: Extended and Sequentially Controllable Drug Release," *ACS Appl Mater Interfaces*, vol. 9, pp. 10567-10576, Mar 29 2017.
- [12] J. D. Mangadla, X. Wang, C. McCleese, M. Escamilla, G. Ramamurthy, Z. Wang, et al., "Prostate-Specific Membrane Antigen Targeted Gold Nanoparticles for Theranostics of Prostate Cancer," *ACS Nano*, vol. 12, pp. 3714-3725, 2018/04/24 2018.
- [13] S. Mignani, J. Rodrigues, H. Tomas, M. Zablocka, X. Shi, A.-M. Caminade, et al., "Dendrimers in combination with natural products and analogues as anticancer agents," *Chemical Society Reviews*, vol. 47, pp. 514-532, 2018.
- [14] Z. Ahmad, A. Shah, M. Siddiq, and H.-B. Kraatz, "Polymeric micelles as drug delivery vehicles," *RSC Advances*, vol. 4, pp. 17028-17038, 2014.
- [15] K. Yang, L. Feng, and Z. Liu, "Stimuli responsive drug delivery systems based on nano-graphene for cancer therapy," *Advanced Drug Delivery Reviews*, vol. 105, pp. 228-241, 2016/10/01/ 2016.
- [16] B. S. Pattni, V. V. Chupin, and V. P. Torchilin, "New Developments in Liposomal Drug Delivery," *Chemical Reviews*, vol. 115, pp. 10938-10966, 2015/10/14 2015.
- [17] N. Kamaly, Z. Xiao, P. M. Valencia, A. F. Radovic-Moreno, and O. C. Farokhzad, "Targeted polymeric therapeutic nanoparticles: design, development and clinical translation," *Chem Soc Rev*, vol. 41, pp. 2971-3010, Apr 7 2012.
- [18] K. Cohen, R. Emmanuel, E. Kisin-Finfer, D. Shabat, and D. Peer, "Modulation of Drug Resistance in Ovarian Adenocarcinoma Using Chemotherapy Entrapped in Hyaluronan-Grafted Nanoparticle Clusters," *ACS Nano*, vol. 8, pp. 2183-2195, 2014/03/25 2014.
- [19] Y. Zhong, F. Meng, C. Deng, and Z. Zhong, "Ligand-directed active tumor-targeting polymeric nanoparticles for cancer chemotherapy," *Biomacromolecules*, vol. 15, pp. 1955-69, Jun 9 2014.
- [20] M. M. Yallapu, S. Khan, D. M. Maher, M. C. Ebeling, V. Sundram, N. Chauhan, et al., "Anticancer activity of curcumin loaded nanoparticles in prostate cancer," *Biomaterials*, vol. 35, pp. 8635-48, Oct 2014.
- [21] H. Wang, H. Yin, F. Yan, M. Sun, L. Du, W. Peng, et al., "Folate-mediated mitochondrial targeting with doxorubicin-polyrotaxane nanoparticles overcomes multidrug resistance," *Oncotarget*, vol. 6, 2014.
- [22] S. Mura, J. Nicolas, and P. Couvreur, "Stimuli-responsive nanocarriers for drug delivery," *Nature Materials*, vol. 12, pp. 991-1003, 2013/11/01 2013.
- [23] X. Zhang, Y. Huang, M. Ghazwani, P. Zhang, J. Li, S. H. Thorne, et al., "Tunable pH-Responsive Polymeric Micelle for Cancer Treatment," *ACS Macro Letters*, vol. 4, pp. 620-623, 2015/06/16 2015.
- [24] B. Jeong and A. Gutowska, "Lessons from nature: stimuli-responsive polymers and their biomedical applications," *Trends in Biotechnology*, vol. 20, pp. 305-311, 2002/07/01/ 2002.
- [25] D. A. Bedoya, F. N. Figueroa, M. A. Macchione, and M. C. Strumia, "Stimuli-Responsive Polymeric Systems for Smart Drug Delivery," in *Advanced Biopolymeric Systems for Drug Delivery*, A. K. Nayak and M. S. Hasnain, Eds., ed Cham: Springer International Publishing, 2020, pp. 115-134.
- [26] L. Zhang, R. Guo, M. Yang, X. Jiang, and B. Liu, "Thermo and pH Dual-Responsive Nanoparticles for Anti-Cancer Drug Delivery," *Advanced Materials*, vol. 19, pp. 2988-2992, 2007.
- [27] C.-Y. Chen, T. H. Kim, W.-C. Wu, C.-M. Huang, H. Wei, C. W. Mount, et al., "pH-dependent, thermosensitive polymeric nanocarriers for drug delivery to solid tumors," *Biomaterials*, vol. 34, pp. 4501-4509, 2013/06/01/ 2013.
- [28] J. R. McDaniel, M. W. Dewhirst, and A. Chilkoti, "Actively targeting solid tumours with thermoresponsive drug delivery systems that respond to mild hyperthermia," *Int J Hyperthermia*, vol. 29, pp. 501-10, Sep 2013.
- [29] D. E. Meyer, B. C. Shin, G. A. Kong, M. W. Dewhirst, and A. Chilkoti, "Drug targeting using thermally responsive polymers and local hyperthermia," *J Control Release*, vol. 74, pp. 213-24, Jul 6 2001.
- [30] M. Gu, X. Wang, T. B. Toh, and E. K. Chow, "Applications of stimuli-responsive nanoscale drug delivery systems in translational research," *Drug Discov Today*, vol. 23, pp. 1043-1052, May 2018.

- [31] S. Bano, F. Ahmed, F. Khan, S. C. Chaudhary, and M. Samim, "Targeted delivery of thermoresponsive polymeric nanoparticle-encapsulated lycopene: in vitro anticancer activity and chemopreventive effect on murine skin inflammation and tumorigenesis," *RSC Advances*, vol. 10, pp. 16637-16649, 2020.
- [32] G. Toniolo, E. K. Efthimiadou, G. Kordas, and C. Chatgililoglu, "Development of multi-layered and multi-sensitive polymeric nanocontainers for cancer therapy: in vitro evaluation," *Scientific Reports*, vol. 8, p. 14704, 2018/10/02 2018.
- [33] M. Rahimi, S. Kilaru, G. E. Sleiman, A. Saleh, D. Rudkevich, and K. Nguyen, "Synthesis and Characterization of Thermo-Sensitive Nanoparticles for Drug Delivery Applications," *J Biomed Nanotechnol*, vol. 4, pp. 482-490, Dec 1 2008.
- [34] C. Kojima, K. Yoshimura, A. Harada, Y. Sakanishi, and K. Kono, "Temperature-sensitive hyperbranched poly(glycidol)s with oligo(ethylene glycol) monoethers," *Journal of Polymer Science Part A: Polymer Chemistry*, vol. 48, pp. 4047-4054, 2010.
- [35] H. C. Besse, A. D. Barten-van Rijbroek, K. M. G. van der Wurff-Jacobs, C. Bos, C. T. W. Moonen, and R. Deckers, "Tumor Drug Distribution after Local Drug Delivery by Hyperthermia, In Vivo," vol. 11, Oct 9 2019.
- [36] B. Banno, L. M. Ickenstein, G. N. Chiu, M. B. Bally, J. Thewalt, E. Brief, et al., "The functional roles of poly(ethylene glycol)-lipid and lysolipid in the drug retention and release from lysolipid-containing thermosensitive liposomes in vitro and in vivo," *J Pharm Sci*, vol. 99, pp. 2295-308, May 2010.
- [37] M. de Smet, S. Langereis, S. van den Bosch, and H. Grüll, "Temperature-sensitive liposomes for doxorubicin delivery under MRI guidance," *J Control Release*, vol. 143, pp. 120-7, Apr 2 2010.
- [38] M. Heskins and J. E. Guillet, "Solution Properties of Poly(N-isopropylacrylamide)," *Journal of Macromolecular Science: Part A - Chemistry*, vol. 2, pp. 1441-1455, 1968/12/01 1968.
- [39] Y. Wenger, R. J. Schneider, 2nd, G. R. Reddy, R. Kopelman, O. Jolliet, and M. A. Philbert, "Tissue distribution and pharmacokinetics of stable polyacrylamide nanoparticles following intravenous injection in the rat," *Toxicol Appl Pharmacol*, vol. 251, pp. 181-90, Mar 15 2011.
- [40] D. Ito and K. Kubota, "Solution Properties and Thermal Behavior of Poly(N-n-propylacrylamide) in Water," *Macromolecules*, vol. 30, pp. 7828-7834, 1997/12/01 1997.
- [41] A. Chilkoti, M. R. Dreher, D. E. Meyer, and D. Raucher, "Targeted drug delivery by thermally responsive polymers," *Advanced Drug Delivery Reviews*, vol. 54, pp. 613-630, 2002/09/13/ 2002.
- [42] W. Liu, B. Zhang, W. W. Lu, X. Li, D. Zhu, K. De Yao, et al., "A rapid temperature-responsive sol-gel reversible poly(N-isopropylacrylamide)-g-methylcellulose copolymer hydrogel," *Biomaterials*, vol. 25, pp. 3005-3012, 2004/07/01/ 2004.
- [43] J. J. Pillai, A. K. T. Thulasidasan, R. J. Anto, D. N. Chithralekha, A. Narayanan, and G. S. V. Kumar, "Folic acid conjugated cross-linked acrylic polymer (FA-CLAP) hydrogel for site specific delivery of hydrophobic drugs to cancer cells," *Journal of Nanobiotechnology*, vol. 12, p. 25, 2014/07/15 2014.